Design and Development of 1-DOF Assisted Physiotherapeutic Device for Rehabilitation of Frozen Shoulder

Atiqa Saleem[1], Shehla Inam[2], Seemab Zakir[2], Leezish Gulshad[2], Faisal Amin[2], Aleena Naweed[2]

[1]Department of Biomedical Engineering, HITECH University, Taxila Cantt, Pakistan

[2]Department of Biomedical Engineering, Riphah International University, Islamabad, Pakistan

*__Correspondence__: atiqa.saleem@hitecuni.edu.pk, shehla.inam@riphah.edu.pk seemabzakir2@gmail.com, leesh.khan@hotmail.com, faisal.amin@riphah.edu.pk, aleenanaweed@gmail.com

Citation | Saleem. A, Inam. S, Zakir. S, Gulshad. L, Amin. F, Naweed. A, "Design and Development of 1-DOF Assisted Physiotherapeutic Device for Rehabilitation of Frozen Shoulder", IJIST, Vol. 07 Special Issue. pp 268-278, May 2025

Received | April 11, 2025 **Revised |** May 13, 2025 **Accepted |** May 15, 2025 **Published |** May 17, 2025.

The growing prevalence of limb-related issues has increased the demand for rehabilitation services. A key focus has been on restoring upper limb functionality and controllability, which are essential for patients to reintegrate into society and improve their quality of life. In this project, a prototype for an assisted physiotherapy device was designed to rehabilitate frozen shoulders. The device supports both external and internal rotation of the shoulder, allowing movement from 0 to 90 degrees. Its adjustable speed control lets patients move their shoulders based on their personal needs and abilities. Additionally, the device provides real-time feedback on the angle, speed, and force applied during rehabilitation. Experimental results show that this prototype is both practical and effective in rehabilitating shoulder rotation.

Keywords: Assisted device, 1 DOF, Frozen shoulder, Rehabilitation, Upper limb

Introduction:

Adhesive shoulder capsulitis, or frozen shoulder, is a condition where excessive scar tissue or adhesions form across the glenohumeral joint, causing pain, stiffness, and limited movement. It can develop either spontaneously (primary or idiopathic adhesive capsulitis) or following shoulder surgery or trauma (secondary adhesive capsulitis) [1]. In a study [2], a novel servomotor joint mobility device for treating frozen was compared to standard therapy. Patients using the device showed significant improvement in shoulder range of motion (ROM- flexion 36 %, abduction 51 %, internal rotation 81 %, and external rotation 88 %) and a 62% decrease pain (measured by VAS). These results outperformed the control group where ROM improvements were more modest, indicating the device's potential as a supplementary treatment for frozen shoulder.

Another study developed a game-based app to help increase patient engagement with home exercises following medical treatment for frozen shoulder. The app, compatible with mobile platforms aimed to improve joint mobility and function through rehabilitation exercises, with prototype testing to ensure it was both user-friendly and motivating. This allowed healthcare professionals to remotely monitor patient progress [3]. In a similar approach, a mobile using Unity 3D was created to simulate frozen shoulder movements, enabling tele-rehabilitation at home. Biofeedback data was sent to physiotherapists providing valuable tool for remote patient management and personalized treatment [4].

Additionally, a wearable motion sensor device paired with a smartphone. App was tested to monitor shoulder ROM. The device showed reliability (ICC range of 0.771 - 0.979) when compared to doctor evaluations and patient using device showed greater shoulder mobility, and functional recovery, than those in a home exercise group, over a three-month period [4]. Another study, involved a three-month home-based program, where patients divided into two groups: smartphone-assisted exercise (n = 42) and traditional self-exercise (n = 42). Both showed significant improvements in ROM and range of motion and pain, but those using smartphones were more satisfied with the technology, suggesting smartphone-assisted were more satisfied with the suggesting smartphone assisted rehabilitation is just as effective and more enjoyable for users [5].

In an interesting participatory study, patients, healthcare providers, game designers, and academics collaborated to refine refined a Kinect-based game to help patients with frozen shoulder move more freely and experience less pain. This iterative process aimed to improve both therapeutic outcomes and the user experience [6]. Another study explored the use of two degree of freedom rehabilitation device specifically patient needing intensive rehabilitation for Adhesive capsulitis [7]. One more study focused on developing an automated sliding CPM device filling a gap in current robotic devices, by offering wide ROM coverage with precise monitoring and affordability for self-exercising patients [8]. Lastly, the effectiveness of shoulder joint mobilization using an innovative servomotor joint mobilization apparatus was examined for frozen shoulder patients [9]. Therefore, this study aims to design and develop a cost-efficient, 1-DOF-assisted device for frozen shoulder rehabilitation, using minimal resources. This device can be used independently by patients or with the help of physiotherapists.

Aim of the study:

These therapeutic exercises are typically guided by a physiotherapist and involve both active and passive movements, depending on the patient's condition. The main goal of rehabilitation devices is to restore a patient's sensory, physical, and psychological abilities, which may have been lost due to injuries, illness, or disease. These devices also help patients compensate for impairments that cannot be fully treated through medical care. Although rehabilitation equipment and techniques are gradually improving, they remain expensive and often come with complex Ranges of Motion (ROM) and high degrees of freedom (DOF).

Many upper-arm exoskeletons rely on human-robot interaction, which can be difficult for patients to operate manually and may lead to high repair and maintenance costs.

In response to these challenges, the authors of this study designed a simple prototype with 1 DOF. This device is easy to use, cost-effective, and locally manufactured, making it more accessible for patients. It helps reduce the cost of physiotherapy sessions while ensuring effective exercise. The device can also be easily used at home. The authors targeted the local community, particularly those who are unable to participate in social activities due to disability or pain.

The ADFFS device can perform 1 DOF movements, such as internal and external shoulder rotations, with four different speed modes, making it simpler to use compared to existing devices. A doctor recommends the appropriate speed, time, and duration for each exercise, so patients only need to select the mode and begin their therapy session. The ADFFS is independent of age, gender, and weight, and it allows physiotherapists to provide precise therapy without the need for manual exercise during multiple sessions. This device promotes progress in rehabilitation by ensuring safety, reliability, and self-dependence for patients.

Methodology:

Directions of AD Device:

This assisted device (AD) was designed to follow the instructions as shown in Figure 1. The AD operates with a 1 DOF movement, allowing for both external and internal shoulder rotation, with shoulder angles ranging from 0° to 90°.

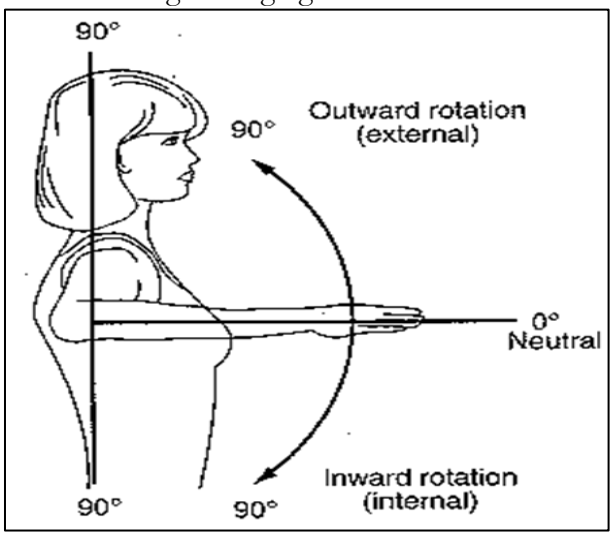

Figure 1. Directions followed by the designed AD

Model Design:

The complete mechanical design was created to support the arm and shoulder, with a graphical user interface (GUI) for mode selection and parameter adjustments. As shown in the block diagram (Figure 2), the assisted device was controlled by the microcontroller through the GUI, allowing the subject to select modes and adjust parameters independently. Sensory feedback was provided for situations where the subject might feel pain or discomfort. In such cases, the subject could stop the device using the safety switch. The device was adjustable to the subject's left arm, while the safety switch was positioned in the right hand for easy access. All operations were controlled by the subject with the microcontroller programming managing mode selection and parameter adjustments.

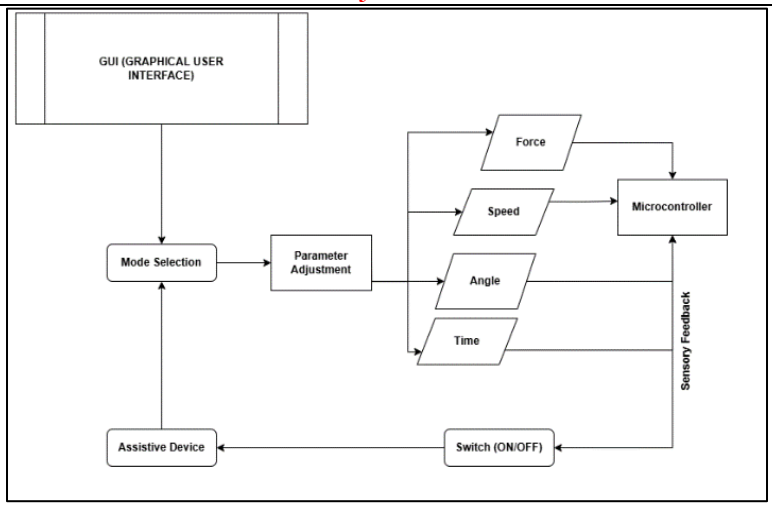

Figure 2. Block diagram of AD

Prototype Design on Solid Edge

The prototype model was designed using Solid Edge software, which provided detailed results to define its purpose. The following diagrams created in Solid Edge included the correct dimensions. Figure 3 shows the dimensions of the prototype's base, which serves as the lower and fundamental part that supports the entire design. These dimensions were selected based on the overall design of the device.

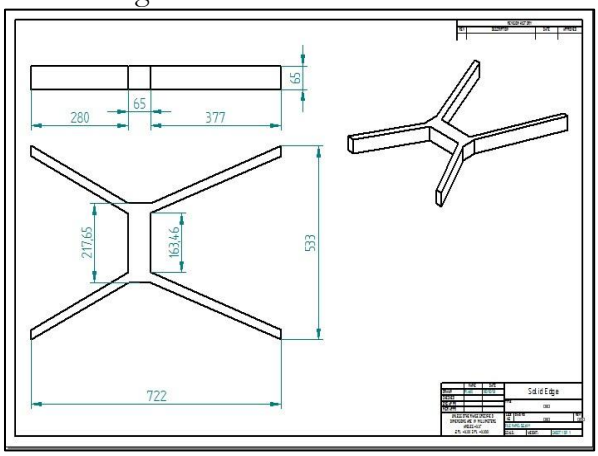

Figure 3. Base of AD

Similarly, Figure 4 illustrates the dimensions of the stainless-Steel rods that support the armrest. The affected arm rests on this part of the device, and the motors move the rods to facilitate exercise of the affected arm.

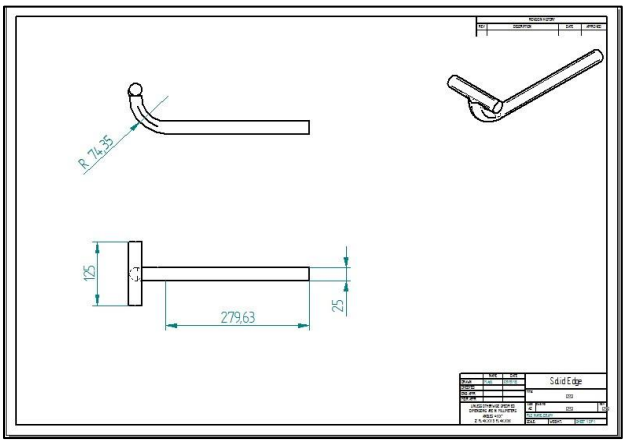

Figure 4. Armrest of AD

The dimensions of the joint that connects the stainless-steel rods are shown in Fig 5. These dimensions were selected to ensure the stability of the device and to make the assisted device comfortable for the patients.

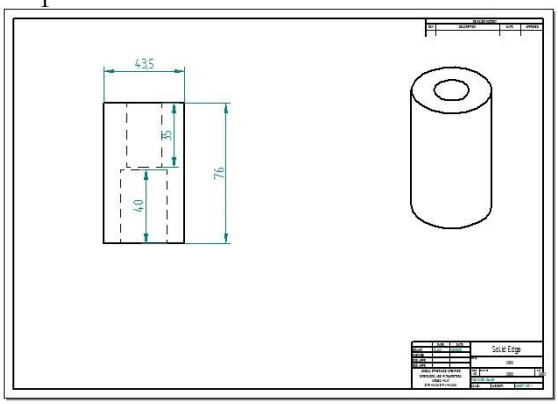

Figure 5. Joint of AD

Figure 6 shows the dimensions of the bending plates, which are perpendicular to the attached rods connecting the standing rods and armrests. Bolts are used to secure the bending plates and rods.

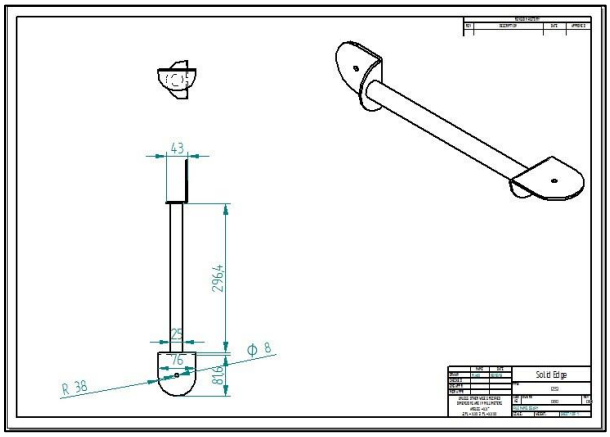

Figure 6. Bend plate of the ADFFS

Figure 7 shows the dimension of the aluminum alloy that adjusts the position of the shoulder and elbow joints. Bent plates with rods were attached to them to the alloy allowing the rods to move either towards or away from the body, thereby enabling movement of the armrest and shoulder.

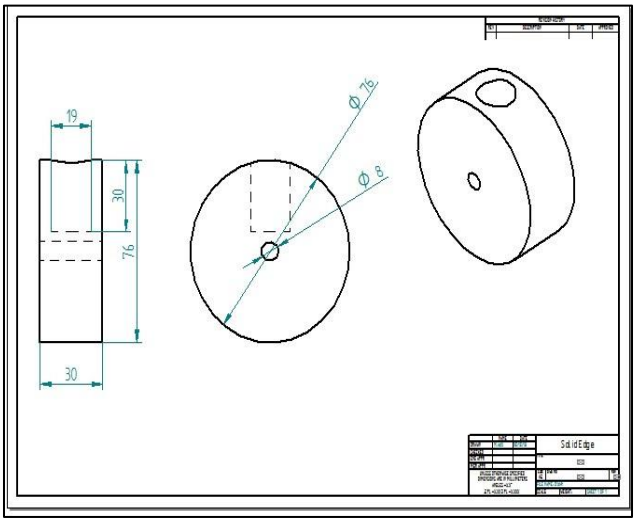

Figure 7. Adjustment of arm part

Motor selection:

DC gear motors were chosen for their ability to provide adjustable speed operations. These motors are ideal for applications that require high starting loads and consistent horsepower, even when operating at 150 % above their base speed. A key advantage of DC gear motors is their ability to generate full torque at low speeds which makes them suitable for carrying the average arm weight (5.3% of total body weight). Given that our prototype design needed to support the weight of the average human arm. The DC gear motor was the optimal choice. Additionally, DC motors offer higher power density, have no field coil in the stator, saving space and are compact. Their design makes them easy to maintain and control with lower inertia making them highly reliable and efficient for our application. Table I shows the specs of DC Gear motor.

Table 1. Motor Specs used in the design (24V DC Gear Motor)

Parameters	DC Gear Motor
Model Type	Model # DME60B6HF-224
Voltage (V)	24.0 V DC
Gear Ratio	1/ 150
Rotation Output (CW/ CCW)	31.3 r/min
Output Speed	300 rpm

Gyroscope and Accelerometer [MPU-6050]:

Sensory devices are used to measure the position and orientation of the device's moving parts. A combination of gyroscope and accelerometer provides a comprehensive array of information. The gyroscope uses the Earth's gravity to measure rotational movement, while the accelerometer detects non-gravitational acceleration. The gyroscope measures the rate of rotation and the accelerometer measures linear vibration. The MPU-6050 sensor used in this study supports a sampling frequency of up to 1 kHz (1000 samples per second). However, in the current setup, the data acquisition was performed at a sampling rate of 100 Hz, which provides a reasonable balance between responsiveness and data stability. A higher sampling rate can offer more precise data, particularly in higher-speed modes where rapid changes in acceleration and angular velocity occur.

In future iterations, increasing the sampling frequency may help reduce data fluctuations and improve the accuracy of recorded force and speed values at higher angles and speeds. Table 2 and Table 3 show the specs of MPU-6050 that used in design.

Table 2. General specifications of mpu-6050

Part/Item	MPU-6050
VDD	2.375V-3.46V
VLOGIC	1.71V to VDD
Serial Interfaces Supported	I^2C
Pin 8	VLOGIC
Pin 9	AD0
Pin 23	SCL
Pin 24	SDA

Table 3. Gyro/MPU-6050 Operating Conditions Used in the Design

Parameters	GYRO/MPU-6050
VDD	2.375-3.46V
VLOGIC	$1.8V_{+}^{-}5\%$ or VDD
Ambient Temperature- T_A	25°C

Choice of Microcontroller:

An Arduino microcontroller was used in this assisted device. The microcontroller was programed to interface with the DC gear motor, enabling it to perform external and

internal rotation of the frozen shoulder at various speeds, ranging from 0 to 90 degrees. The Arduino's PWM pins were connected to the L298n motor driver module, while the analog pins were linked to the motor. The power (V), and ground (GND) connections were made to the adaptor's GND and power. These components work together to operate the prototype and the physiotherapeutic device (Figure 8).

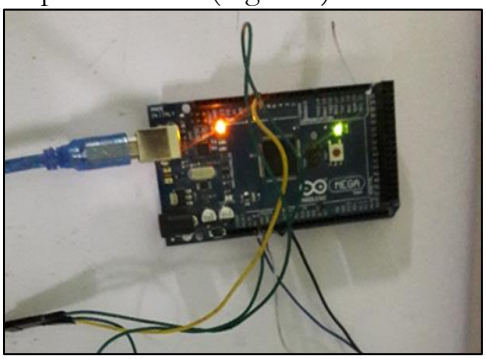

Figure 8. Arduino (mega 2560)

Power Supply and Calculation of Force:

The power supply for the device was connected to a drive circuit that provided 12 volts to the DC gear motor, as the motor operates on 12 volts. Two sensors, a gyroscope and an accelerometer [MPU-6050], were used to measure acceleration, which was then used to calculate the force generated by the device in moving the armrest. The following formula was used for the calculation:

$$F = ma \qquad (1)$$

Where "a" is the acceleration, and "m" represents the mass of the arm. All necessary coding was completed using the Arduino Mega microcontroller to control the motor's speed. Switch buttons were incorporated to turn the device ON/OFF and adjust the speed, force, and angle based on the patient's needs.

Implementation of prototype:

Metal fabrication was done to build some metal structures by cutting, bending, and assembly processes. The base of the design was made of mild steel, size of 2"× 1", 16 gauges. Caster wheels were attached to the lower side of the base for movement from one place to another. Electric arc welding was used to prepare this mechanical design. For circular joints 'Lathe Machine' was used. The dimensions of the Stainless-steel rod were 18 gauges, 18mm. The bending plate used in joints was of mild steel with a diameter of 3.6mm. Screws were made up of aluminum alloy, sizes of 4mm and 8mm. Joints were also made up of aluminum. The vertical rod's diameter was 1", 16-gauges, the height of 4". The finished form of the device parts after fabrication is given below in Figure 9.

Figure 9. Final design of prototype

Results:

The speed and force exerted by the assisted device in moving the armrest were measured at angles of 15°, 30°, 45°, 60°, and 75°. The device was programmed to operate in four modes. Mode 1 was the slowest, moving the armrest at a low speed with minimal force. Modes 2, 3, and 4 gradually increased the speed and force, with Mode 2 offering moderate speed and force, Mode 3 providing high speed and force, and Mode 4 delivering the highest speed and force. The results for all four modes (1–4) at the angles of 15°, 30°, 45°, 60°, and 75° are summarized in Table IV.

Table 4. Observed speeds and forces at different angles and modes

	Mode (Slow)					
Angle (◦)	15^0	30^0	45^0	60^0	75^0	90^0
Speed (deg/s)	31.5	45.0	53.2	77	89	110
Force (Fv)	47	56	102	69	134	157
	Mode (Moderate)					
Angle (◦)	15^0	30^0	45^0	60^0	75^0	90^0
Speed (deg/s)	42	59.0	73.2	89	111	179
Force (Fv)	57	68.1	74.8	88.7	122.3	163
	Mode (High)					
Angle (◦)	15^0	30^0	45^0	60^0	75^0	90^0
Speed (deg/s)	55	45.0	86.2	99.1	131	185
Force (Fv)	62.5	74.9	88.2	97.8	139	187
	Mode (Very high)					
Angle (◦)	15^0	30^0	45^0	60^0	75^0	90^0
Speed (deg/s)	64.5	87.0	120	147.3	151	110
Force (Fv)	73	90.30	104.1	149.7	169.9	197.32

Acquired Data Representation:

The acquired data showed that force and speed increased at higher angles. As the angle of the armrest increased from 15° to 90°, more force was needed to lift the arm. The angular rotational speed was recorded in degrees per second (deg/s), showing the speed at each respective angle. After the collection of data, a clear trend of increasing force at different armrest angles was observed. The data was graphically presented for all four modes (1-4). Overall, the trend indicated that at higher modes, more force was required to move the armrest. However, a limitation of this device was that sometimes the same values for force and speed were observed at the same armrest angles.

Explanation of Results:

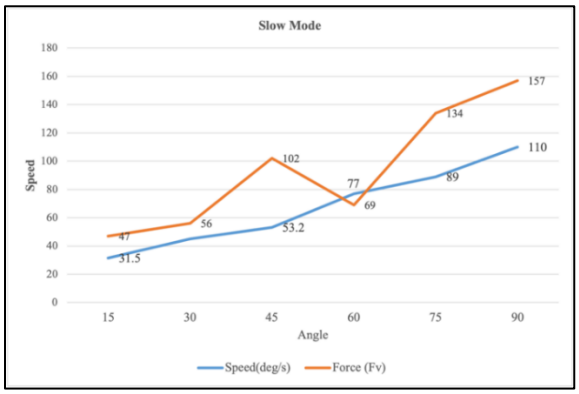

Figure 10. Slow mode of AD

Figure 10 shows the graph of force, angle, and speed at Slow Mode 1. This mode worked as the baseline, as it operates at the lowest speed and force. It effectively demonstrated the device's ability to gently mobilize the shoulder, which is crucial for early

rehabilitation stages or patients with high pain sensitivity. The linear increase in force and speed with angle suggests predictable mechanical behavior, indicating good calibration and safe motion for initial therapy sessions. It demonstrates that as speed increased, force also increased to reach higher angles. Although there were some fluctuations in the readings, the overall graph indicated that these three parameters are directly related. As the angle increased from 15° to 90°, the speed started at 31.5 deg/s, gradually increased to 77 deg/s at 60°, and peaked at 110 deg/s at 90°. Meanwhile, the force began at 47 Fv, steadily increased to 134 Fv at 75°, and reached 157 Fv at 90°. This shows that both speed and force increased consistently with the angle, with speed rising slightly faster than force at higher angles.

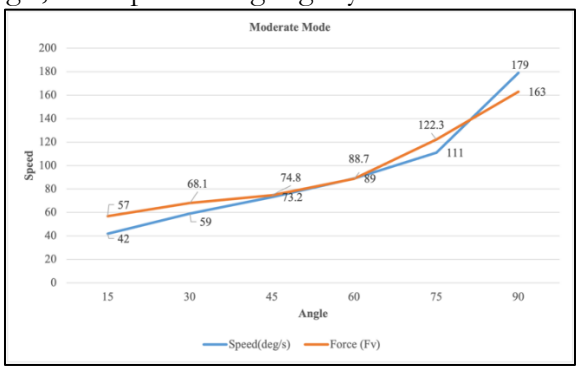

Figure 11. Moderate mode of AD

Similarly, Figure 11 shows the graph for Moderate Mode 2, where the speed values were higher as compared to the Slow Mode. Mode 2 exhibited a steeper increase in both force and speed compared to Mode 1. This implies a significant jump in mechanical demand, suitable for mid-stage therapy. The sharper slope in speed may suggest that the motor reaches a higher torque efficiency in this mode. It also indicates that patients with moderate mobility can be safely progressed to this mode, but with continuous monitoring to prevent strain. When the speed is greater the applied force increases with it and so are the selected angles. As a result, both force and speed were greater, but the increasing trend remained the same as in Slow Mode. As the angle increased from 15° to 90°, the speed started at 42 deg/s, gradually increased to 89 deg/s at 60°, and then peaked at 179 deg/s at 90°. Meanwhile, the force began at 57 Fv, steadily increased to 122.3 Fv at 75°, and reached 163 Fv at 90°. This demonstrated that both speed and force increased consistently with increased angle. We also observed that the speed raised slightly faster than force at higher angles.

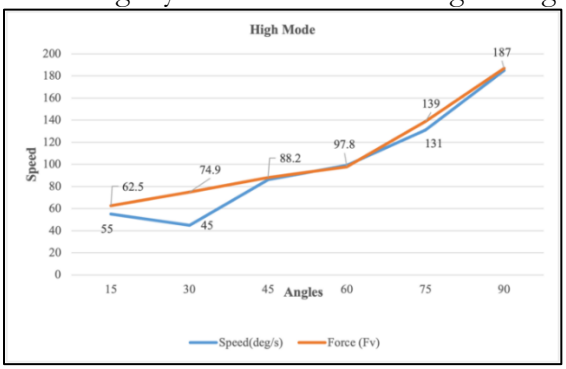

Figure 12. High mode of AD

Figure 12 shows the graph of force, speed, and angles at High Mode. This mode pushed the motor towards its upper performance threshold. The force and speed values increased more aggressively, and small fluctuations began to appear in the data. These fluctuations could indicate either sensor limitations at higher speeds or minor mechanical inconsistencies. Clinically, this mode might be appropriate for strengthening or improving endurance, but caution is advised due to potential fatigue or overstimulation. When High

Mode 3 was selected, the device began moving at high speed with high force, reaching the 90-degree angle. As the angle increased from 15° to 90°, the speed started at 42 deg/s, gradually increased to 111 deg/s at 75°, and peaked at 187 deg/s at 90°. Meanwhile, the force started at 62.5 Fv, steadily increased to 139 Fv at 75°, and reached 187 Fv at 90°. This demonstrated that both speed and force increased consistently with the increased angle, however the speed rised somewhat faster than force at higher angles.

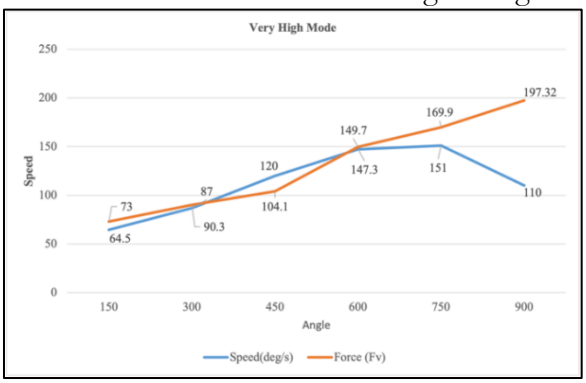

Figure 13. Very high mode of AD

Figure 13 shows the graph for Very High Mode 4. In this mode, the speed was very high, and the armrest moved quickly. In this mode, the device operated at or near its maximum output. Notably, the drop in speed at 90° despite rising force suggests either a limitation in motor torque or a lag in sensor response. This anomaly highlights the importance of evaluating both mechanical and sensor thresholds. From a therapeutic standpoint, Mode 4 may be reserved for final-stage rehabilitation or athletic patients, and should be used under supervision due to increased variability. As the angle increased from 15° to 90°, the speed started at 64.5 deg/s, peaked at 149.7 deg/s at 60°, and then decreased to 110 deg/s. Meanwhile, the force steadily increased from 73 Fv at 15° to 197.32 Fv at 90°. This suggests that while speed initially increased with the angle up to a point before decreasing, force continued to increase consistently across the entire range of angles. However, the last speed value appears to be incorrect, possibly due to human error, although all other values followed the increasing trend of force with angle.

Discussion:

The results from this study followed a similar pattern to what has been seen in previous research on 1-DOF rehabilitation devices for frozen shoulder. Like the studies by Kim et al. (2018) and Zhang et al. (2019), it was found that as the assisted device moved the arm at higher angles, both the force and speed required were increased. This supports the idea that gradually increasing resistance and movement speed can help improve joint mobility over time. One thing that sets this study apart is the detailed mechanical design and data recording. While earlier research focused mostly on patient outcomes like pain relief or range of motion, we looked closely at how the device actually performed at different angles and settings. This gave a clearer picture of how force and speed changed in real time, which could be useful when refining or adjusting device performance in the future.

That said, we did notice a few inconsistencies—especially at 90° in the Very High Mode, where the speed unexpectedly dropped. This was likely due to a sensor glitch or human error during data collection. It's a reminder that even with a well-functioning device, accurate measurement tools are just as important. In fact, the issue may also be linked to the sampling frequency of the sensors. In faster modes, where the device moves more quickly, a low sampling rate might miss sudden changes in speed or force, leading to incomplete or inconsistent data. Using a higher sampling frequency could help capture more accurate results and give a better understanding of how the device performs under different conditions. It's something worth improving in future versions of the setup.

Conclusion:

In conclusion, the assisted device for frozen shoulder rehabilitation was designed to facilitate therapeutic exercises for patients with limited upper limb mobility. It supports up to 5.3% of the total body weight and accommodates a wide range of ages. The user-friendly design allows the device to be controlled with the patient's non-affected hand, ensuring safety with an immediate stop mechanism in case of discomfort. The device offers one degree of freedom for internal and external shoulder rotations across four speed levels, which can be selected based on medical recommendations for optimal therapy. This enables patients to manage their rehabilitation independently at home, regardless of age, gender, or weight, while also assisting physiotherapists in delivering precise and consistent therapy without physical intervention.

References:

[1] K. L. Wu, Y. H. Wang, Y. C. Hsu, Y. C. Shu, C. H. Chu, and C. A. Lin, "Developing a Motion Sensor-Based Game to Support Frozen Shoulder Rehabilitation in Older Adults through a Participatory Design Approach," *Games Health J.*, Oct. 2024, doi: 10.1089/G4H.2023.0097;JOURNAL:JOURNAL:G4H;PAGE:STRING:ARTICLE/CHAPTER.

[2] S. Inam, F. Amin, H. Al Faisal, M. Waqar, R. Ehsan, and U. Iftikhar, "Enhancing Rehabilitation for Frozen Shoulder With a Two-Degree of Freedom Approach," *6th Int. Conf. Robot. Autom. Ind. ICRAI 2024*, 2024, doi: 10.1109/ICRAI62391.2024.10894255.

[3] 이제우, "Development and Evaluation of a Sliding Type Continuous Passive Motion Automation Device for Diagnosis and Rehabilitation of Frozen Shoulder," *Diss. 서울대학교 대학원*, 2023.

[4] S.-D. L. Cheng-Ju Wu, Hua Ting, Chuan-Chao Lin, Yi-Chung Chen, Ming-Che Chao, "Efficacy of Joint Mobilization Apparatus in Treating Frozen Shoulder," *Appl. Sci.*, vol. 11, no. 9, p. 4184, 2021, doi: https://doi.org/10.3390/app11094184.

[5] Y. Choi, J. Nam, D. Yang, W. Jung, H. R. Lee, and S. H. Kim, "Effect of smartphone application-supported self-rehabilitation for frozen shoulder: a prospective randomized control study," *Clin. Rehabil.*, vol. 33, no. 4, pp. 653–660, Apr. 2019, doi: 10.1177/0269215518818866,.

[6] N. Chiensriwimol, P. Mongkolnam, and J. H. Chan, "Frozen shoulder rehabilitation: Exercise simulation and usability study," *ACM Int. Conf. Proceeding Ser.*, pp. 257–264, Dec. 2018, doi: 10.1145/3287921.3287951;PAGE:STRING:ARTICLE/CHAPTER.

[7] S. G. Thomas Stütz, Gerlinde Emsenhuber, Daniela Huber, Michael Domhardt, Martin Tiefengrabner, Gertie Janneke Oostingh, Ulrike Fötschl, Nicholas Matis, "Mobile Phone–Supported Physiotherapy for Frozen Shoulder: Feasibility Assessment Based on a Usability Study," *JMIR Rehabil Assist Technol*, vol. 4, no. 2, 2017, doi: 10.2196/rehab.7085.

[8] H. V. Le, S. J. Lee, A. Nazarian, and E. K. Rodriguez, "Adhesive capsulitis of the shoulder: review of pathophysiology and current clinical treatments," *Shoulder Elb.*, vol. 9, no. 2, pp. 75–84, Apr. 2017, doi: 10.1177/1758573216676786.

[9] C. E. Chung and C. H. Chen, "The App Game Interface Design for Frozen Shoulder Rehabilitation," *Adv. Intell. Syst. Comput.*, vol. 486, pp. 507–516, 2017, doi: 10.1007/978-3-319-41685-4_45.